Mihajlo Aranđelović[1], Simon Sedmak[1], Radomir Jovičić[1], Srđa Perković[2], Zijah Burzić[2], Branislav Đorđević[1], Zoran Radaković[3]*

NUMERICAL SIMULATION OF WELDED JOINT WITH MULTIPLE VARIOUS DEFECTS

NUMERIČKA SIMULACIJA ZAVARENOG SPOJA SA VIŠE RAZLIČITIH GREŠAKA

Originalni naučni rad / Original scientific paper
UDK /UDC:

Rad primljen / Paper received: 15.3.2021

Adresa autora / Author's address:
[1)] University of Belgrade, Innovation Centre of the Faculty of Mechanical Engineering, Belgrade, Serbia
email: simon.sedmak@yahoo.com
[2)] Military Technical Institute, Belgrade, Serbia
[3)] University of Belgrade, Faculty of Mechanical Engineering, Belgrade, Serbia

Keywords
- welding defects
- finite element method (FEM)
- steel S235JR
- tensile test

Ključne reči
- greške u zavarenim spojevima
- metoda konačnih elemenata (MKE)
- čelik S235JR
- ispitivanje zatezanjem

Abstract

The paper presents continuation of extensive work on determining the behaviour of welded joints in the presence of multiple various types of defects, a problem that is not sufficiently covered by existing standards, such as EN ISO 5817 series. The research involves the development of numerical models, based on real geometries of welded joints made of typical structural steel S235JR, along with experimental tests that would verify the models, and provide additional insight into the behaviour of the welded structure under such unusual conditions. For this purpose, welding defects most likely to occur in practice are selected, and a number of their combinations is produced intentionally in welded plates. The goal of the numerical models is to determine the most critical locations in terms of stresses, and to analyse their integrity in the presence of cracks. While the experiments did validate the majority of numerically obtained results, there are certain unexpected differences. This provides the authors with additional goals of determining why these differences occur. For this purpose, additional destructive tests are performed, revealing the cause behind the disagreement between real and numerical results, while also confirming authors' suspicions.

Izvod

U radu je prikazan deo obimne analize ponašanja zavarenih spojeva sa istovremenim prisustvom nekoliko različitih vrsta grešaka u zavarenom spoju, što predstavlja problem koji nije pokriven postojećim standardima, poput EN ISO 5817 serije. Predstavljeno istraživanje obuhvata razvoj numeričkih modela na osnovu stvarne geometrije zavarenih spojeva izvedenih od klasičnih konstrukcionih čelika tipa S235JR, kao i eksperimentalna ispitivanja u cilju verifikacije ovih modela i dobijanja dodatnog uvida u ponašanje zavarenih konstrukcija u ovakvim neuobičajenim uslovima. U tu svrhu su odabrane one vrste grešaka koje se najčešće javljaju u zavarivačkoj praksi, i različite kombinacije ovih grešaka su namenski unete u zavarene spojeve. Cilj numeričkih modela je u određivanju najkritičnije lokacije u pogledu napona, i analiza njihovog integritet u prisustvu prslina. Iako su eksperimenti potvrdili većinu numeričkih rezultata, uočene se neke neočekivane razlike. Ovim se pred autorima postavlja novi cilj, određivanje uzroka ovih razlika. U tu svrhu su urađena dodatna ispitivanja razaranjem, kojima je utvrđen stvarni razlog neslaganja numeričkih i eksperimentalnih rezultata, čime su početne sumnje autora potvrđene kao ispravne.

INTRODUCTION

Defects in welded joints often occur as a result of several factors, including geometry, welding process and metallurgy. The goal of existing standards /1, 2/ is to keep defects below the acceptable limits. These limits, however, are only defined for individual defect types (or a group of same defects, e.g. clustered porosity), and do not consider the presence of multiple different defects. There are several combinations of such defects that can occur in welded structures, and the goal of this research (a part of the doctoral thesis of the paper's first author) is to investigate how these different combinations affect structural integrity of the welded joint.

The research consists of several stages, including welding itself, numerical simulations (frequently used in this type of analyses), /3-6/, and various tests (such as tensile tests and fractography) /7-10/. Initial behaviour of numerical models is compared to the tensile test, and certain differences are observed in one group of specimens. This inspired the authors to determine the reason, since such scenarios are typically not encountered during simulations. For this purpose, the fractured surfaces of specimens obtained after tensile tests are observed. The initial assumption is that the cause of differences in numerical and real results is the presence of a previously undetected internal defect (the intentionally caused ones are all surface type), and this is proven to be correct. The final stage then involves the adaptation of the existing numerical model to the real state, including the newly discovered defect. This provides more accurate results with good agreement with the experiment, in terms of behaviour during fracture.

MATERIALS, WELDING PREPARATION AND PROCEDURE

Welded plates are produced of S235JR steel as the parent material. This is a non-alloyed structural steel widely used in all industrial fields /11-14/, mainly due to its cost effectiveness and good weldability. This material is selected for the initial stage in order to verify whether the adopted testing method works sufficiently well. Future research will focus on applying this methodology to other steels of higher quality. S235 grade offers respectable mechanical properties (yield stress and tensile strength). The letter 'S' in S235JR stands for structural, '235' represents yield stress, i.e. minimal value of 235 N/mm², and 'JR' represents guaranteed toughness of 27 J at room temperature.

Defect combinations include excess weld metal, undercuts, incomplete root penetration, vertical misalignments, and weld metal sagging, /15/. Among these, misalignment is assumed to be the most influential, and it is produced in two (out of four) combinations. One of these combinations is the problem, as its results differ between tensile tests and numerical simulations.

Tables 1 and 2 show the chemical composition and mechanical properties of the steel, respectively, used as input data for numerical simulations.

Table 1. Chemical composition of steel S235JR.

Element	C	Mn	P	S	N	Cu
Percentage	0.17	1.4	0.035	0.035	0.12	0.55

Table 2. Mechanical properties of steel S235JR.

Material	Yield stress, R_{eH} (MPa)	Tensile strength R_m (MPa)	Thickness (mm)
S235JR	235	360-510	12

As for the filler material, the VAC 60 /16/ wire is used, typically used for welding non-alloyed and low-alloyed steels with yield stress up to 530 MPa, while also being widely available. Additionally, it offers good plasticity, improving the integrity of welded joints. Its chemical composition and mechanical properties are shown in Tables 3 and 4.

Table 3. Mechanical properties of VAC 60.

Material	Yield stress R_{eH} (MPa)	Tensile strength R_m (MPa)	Elong. (%)	Toughness at -40°C (J)
VAC 60	> 410	510-590	> 22	> 47

Table 4. Chemical composition of VAC 60.

Element	C	Si	Mn	P	S
(%)	0.08	0.9	1.5	< 0.025	< 0.025

Metal Active Gas (MAG) welding procedure is selected in this case, since the materials used do not have any specific requirements due to their low-alloyed nature, and the procedure is relatively simple to set-up and perform, while being efficient in terms of heat input. As is common practice with this procedure /16/, the M21 gas mixture is used, consisting of 82% argon and 18% carbon-dioxide. Relevant welding parameters, including current, voltage and welding speed, are all given in Tables 5 and 6. Table 5 refers to plates without misalignment, whereas Table 6 shows parameters for plates with 2 mm misalignment. Heat input in this table is calculated in accordance with the well-known formula, /17/, whereas all of the parameters are recorded using Kemppi ARC Q /18/ device (Fig. 1):

$$Q = \frac{\eta I U}{v_z \cdot 1000} = 1.25 \ \frac{\text{kJ}}{\text{mm}}, \qquad (1)$$

where: Q is heat input; I is the current; U is voltage; v_z is the welding speed; and η is welding procedure efficiency (0.9 in the case of MAG procedure).

Table 5. Welding parameters for joints without misalignment.

Layer	Interpass temp. (°C)	Current (A)	Voltage (V)	Weld. speed (mm/s)	Heat input (kJ/mm)
Root	< 150	111	19.3	2.2	0.87
Fill 1	< 150	141	23.9	3.2	0.95
Fill 2	< 150	150	22	4.1	0.71

Table 6. Welding parameters for joints with misalignment.

Layer	Interpass temp. (°C)	Current (A)	Voltage (V)	Weld. speed (mm/s)	Heat input (kJ/mm)
Root	< 150	91	18.8	1.7	0.91
Fill 1	< 150	110	19.4	2.6	0.74
Fill 2	< 150	120	19.8	1.9	1.12

Figure 1 also shows the preparation of plates (500× 300 mm) for welding, with groove edges 60°, and width around 2 mm. It should be noted that the plates are cut in the direction perpendicular to rolling.

Figure 1. Kemppi Arc Q device used for monitoring of welding parameters (top), and S235JR plates with misalignment being prepared for welding (bottom).

TENSILE TESTING AND COMPARISON WITH INITIAL NUMERICAL SIMULATIONS

The experimental part of the investigation consists of tensile tests performed at the Military Technical Institute in Belgrade, Serbia, using an INSTRON tensile test machine with loading capacity of 250 kN (25 tonnes), Fig. 2. Taking

into account the cross-section of the specimens that are cut out of the welded plates (250×10 mm) and the assumed mechanical properties of S235JR steel, it is expected that failure should occur at around 90-95 kN, more or less confirmed by the experiment. It is important to note that all specimens are cut from the plate without any additional machining in order to maintain their 'unusual' geometry resulting from the defects. Figure 3 shows specimens before the test, divided into four groups, depending on the defects, and Fig. 4 shows one of the obtained stress-strain diagrams, for the case of misalignment, excess weld metal, undercut and incomplete root penetration. The diagram, of course, is obtained based on the force-displacement curve from the tensile test itself.

Figure 2. INSTRON tensile test machine of 250 kN capacity.

The numerical model is shown in Fig. 5, and it is created in Abaqus® 2017, a software package frequently used for finite element analyses in a wide range of different scientific and industrial fields, including fatigue, /19-26/.

Figure 3. Tensile test specimens (all four groups).

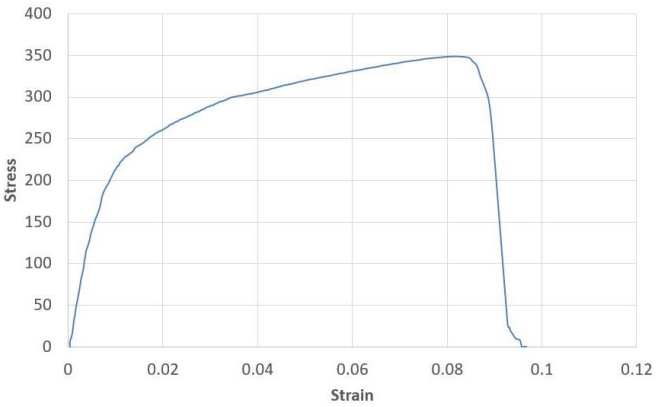

Figure 4. Results of tensile tests for the second group of specimens (excess WM, undercut, incomplete root penetration).

All defects are measured on existing specimens and their dimensions are used in the models as well. Input data for the calculation, which involves the determining of stress state under the assumption of elastic and plastic behaviour (in the case of any plastic strain present), are taken from diagrams as the one shown in Fig. 4. These parameters include yield stress, tensile strength, and strain values at these points.

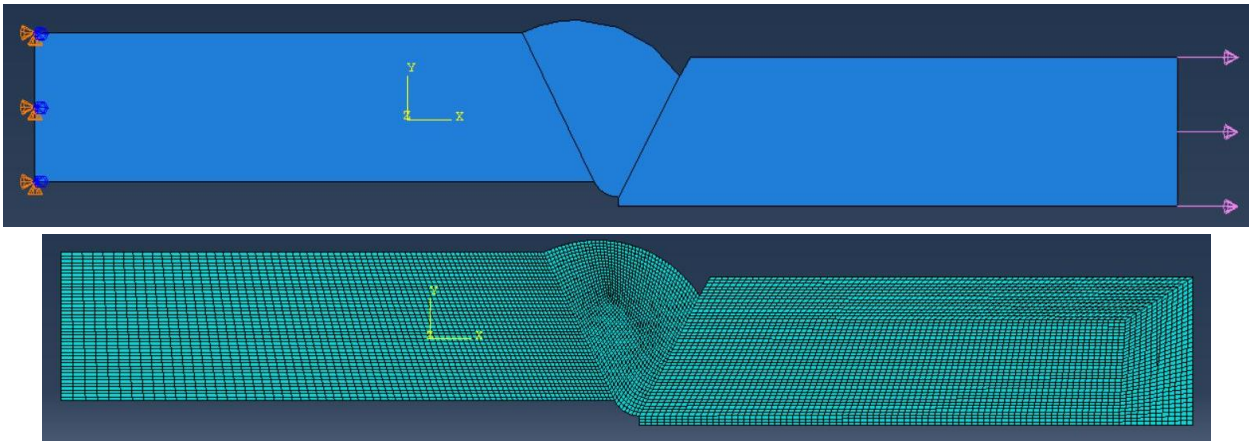

Figure 5. Finite element model of the specimen with misalignment, excess WM, undercut and incomplete root penetration: boundary conditions (upper figure, left) and tensile load (upper figure, right), and finite element mesh (lower image).

Boundary conditions and loading are defined to simulate experimental conditions in the tensile test machine – one end of the specimen is fixed, whereas the other is subjected to a tensile load. The tensile load in this case is 100 MPa, since it is assumed it can cause plastic strain in some models. The mesh contains standard linear quad finite elements CPS4R. Elements near areas of the highest expected stresses and strains (in and around the weld metal) are smaller in size in order to improve the accuracy of the obtained results and ensure convergence. For this reason, several different finite element sizes are tested iteratively, as is common practice when generating the mesh for these models.

Figure 6 shows the results for stress distribution in the numerical model. From this image, it can be concluded that the undercut in the weld face and the part of the weld root which would correspond to the fusion line/heat affected zone, on the upper plate side (in terms of misalignment) are the most critical locations, as the stress levels in these regions exceed the parent material yield stress (around 236 MPa).

Figure 7 shows behaviour of a specimen from this group, during the different stages of the tensile test. By comparing Figs. 6 and 7, it can be seen that there is a difference in stress concentration on the root side - in the numerical model, the crack would initiate on the upper plane side, whereas, in reality the crack initiates on the other side, near the lower plane. In both cases, significant plastic strain also occurs in the undercut, initiating another crack immediately before failure. This outcome raises additional questions.

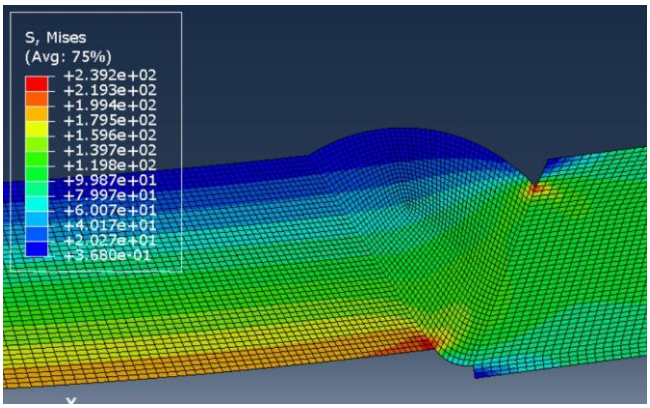

Figure 6. Stress distribution in the numerical model, with two prominent stress concentration locations (the weld root and the face undercut).

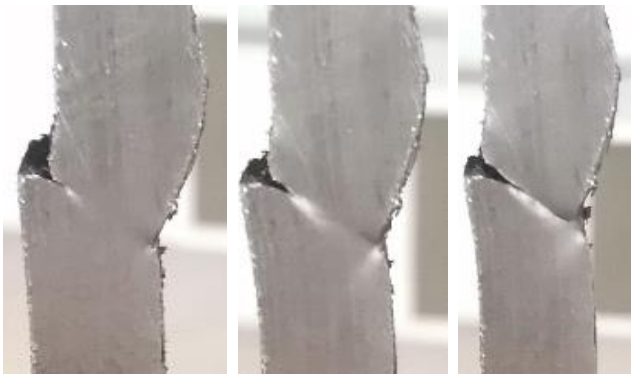

Figure 7. Welded joint specimen under tensile loads at different stages of the experiment.

By examining the fracture surfaces of welded joint specimens after the tensile testing, the authors' suspicions are confirmed - as can be seen in Fig. 8. There is indeed a lack of fusion in the assumed location, represented by the much darker surface in the figure.

The first assumption is that there could be more defects present than originally intended, since all of the deliberate defects are on the surface. Because of the way the root weld is performed, it is assumed it includes an additional defect, the lack of fusion. This would imply that the actual load-bearing cross-section of the specimen in the region including the weld metal and the lower plate would be much smaller, thus resulting in higher stress levels. Lack of fusion is 'blamed' for the experimental result, since the welder could not properly reach the root due to the decreased gap as the plates deform due to heat input, along with the fact that the welder had to focus on the other plate, in order to decrease the heat input in this region, for the purpose of creating incomplete penetration of root.

Figure 8. Model with excess weld metal, incomplete root penetration and an undercut.

CONCLUSIONS

The main goal in this paper is to investigate the behaviour of welded joints with multiple simultaneous defects (of different kinds), using numerical simulations and experimental methods. It is determined that there is disagreement in one of the models and welded joint specimens with a specific combination of defects. This presented the authors with a new goal - to determine the reason for this unexpected difference.

It is assumed that the presence of lack of fusion on the root side of the welded joint is responsible, i.e. that an additional defect, which cannot be detected using surface non-destructive test methods, had caused the unexpected fracture behaviour. Once the fracture surfaces were analysed following the experiments, this hypothesis is confirmed.

This suggests that there are more factors that need to be taken into account when considering the effects of multiple defects on welded joint integrity, and that tensile tests alone are not always sufficient as a form of verification. Instead, additional methods, related to the microstructure and fracture surface should also be included, in order to obtain proper insight into the results.

This research represents the introduction for a more complex analysis, which will be conducted in the near future. This analysis will include the development of new and improved numerical models, based on the knowledge of internal welding defects obtained in this research. The

goal will be to obtain a numerical model that will show a more similar behaviour during tensile loading and, especially, fracture.

REFERENCES

1. SRPS EN ISO 5817:2015, Institute for Standardization of Serbia, 2015.
2. Sedmak, S., Jovičić, R., Sedmak, A., et al. (2018), *Influence of multiple defects in welded joints subjected to fatigue loading according to SIST EN ISO 5817: 2014*, Struct. Integ. and Life, 18(1): 77-81.
3. Jovičić, R., Sedmak, S., Tatić, U., et al. (2015), *Stress state around imperfections in welded joints*, Struct. Integ. and Life, 15(1): 27-29.
4. Sedmak A. (2018), *Computational fracture mechanics: An overview from early efforts to recent achievements*, Fatig. Fract. Eng. Mater. Struct. 41(12): 2438-2474. doi: 10.1111/ffe.12912
5. Kirin, S., Sedmak, A., Zaidi, R. et al. (2020), *Comparison of experimental, numerical and analytical risk assessment of oil drilling rig welded pipe based on fracture mechanics parameters*, Eng. Fail. Anal. 114: 14600. doi: 10.1016/j.engfailanal.2020.104600
6. Jeremić, L., Sedmak, A., Petrovski, B., et al. (2020), *Structural integrity assessment of welded pipeline designed with reduced safety*, Tech. Gazette 27(5): 1461-1466. doi: 10.17559/TV-20200413142538
7. Jovičić, R., Sedmak, A., Prokić-Cvetković, R., et al. (2011), *Cracking resistance of AlMg4.5Mn alloy TIG welded joints*, Struct. Integ. and Life, 11(3): 205-208.
8. Fernandino, D.O., Tenaglia, N., Boeri R.E., et al. (2020), *Microstructural damage evaluation of ferritic-ausferritic spheroidal graphite cast iron*, Fratt. ed Integ. Strutur. 51: 477-485, doi: 10.3221/IGF-ESIS.51.36
9. Sedmak, S., Aranđelović, M., Jovičić, R., et al. (2020), *Influence of cooling time t8/5 on impact toughness of P460NL1 steel welded joints*, Adv. Mater. Res. 1157: 154-160. doi: 10.4028/www.scientific.net/AMR.1157.154
10. Medjo, B., Rakin, M., Gubeljak, N., et al (2015), *Failure resistance of drilling rig casing pipes with an axial crack*, Eng. Fail. Anal. 58: 429-440. doi: 10.1016/j.engfailanal.2015.05.015
11. Somodi, B., Kövesdi, B. (2018), *Residual stress measurements on welded square box sections using steel grades of S235-S960*, Thin-Walled Struct. 123: 142-154. doi: 10.1016/j.tws.2017.11.028
12. Correia, J.A.F.O., da Silva, A.L.L., Xin, H., et al. (2021), *Fatigue performance prediction of S235 base steel plates in the riveted connections*, Structures 30: 745-755. doi: 10.1016/j.istruc.2020.11.082
13. Winczek, J. (2016), *Modeling of heat affected zone in multipass GMAW surfacing S235 steel element*, Procedia Eng. 136: 108-113. doi: 10.1016/j.proeng.2016. 01.182
14. Kristensen, J.K. (2009), *Thick plate CO_2-laser based hybrid welding of structural steels*, Weld. World, 53: 48-57. doi: 10.1007/BF03266691
15. Boaretto N., Centeno T.M. (2017), *Automated detection of welding defects in pipelines from radiographic images DWDI*, NDT & E Int. 86(C): 7-13, doi: 10.1016/j.ndteint.2016.11.003
16. Sedmak, S.A., Burzić, Z., Perković, S., et al. (2019), *Influence of welded joint microstructures on fatigue behaviour of specimens with a notch in the heat affected zone*, Eng. Fail. Anal. 106: 104162. doi: 10.1016/j.engfailanal.2019.104162
17. Merchant, S.Y. (2015), *Investigation on effect of heat input on cooling rate and mechanical property (hardness) of mild steel weld joint by MMAW process*, Int. J Modern Eng. Res. 5(3): 34-41.
18. https://www.kemppi.com/en-US/
19. Choshnova, D. (2010), *The structure of stream and temperature distribution in the reaction shaft of the flash smelting furnace - computer simulation*, Struct. Integ. and Life, 10(2): 129-133.
20. Milovanović, A., Sedmak, A., Čolić K., et al. (2017), *Numerical analysis of stress distribution in total hip replacement implant*, Struct. Integ. and Life, 17(2): 139-144.
21. Đorđević, B., Sedmak, S., Tanasković, D., et al. (2021), *Failure analysis and numerical simulation of slab carrying clamps*, Frattura ed Integ. Strut. 15(55): 336-344. doi: 10.3221/IGF-ESIS.55.26
22. Grbović, A., Kastratović, G., Sedmak, A., et al. (2019), *Determination of optimum wing spar cross section for maximum fatigue life*, Int. J Fatigue 127: 305-311. doi: 10.1016/j.ijfatigue.2019.06.019
23. Chang, P.H., Teng, T.L. (2004), *Numerical and experimental investigations on the residual stresses of the butt-welded joints*, Comp. Mater. Sci. 29(4): 511-522. doi: 10.1016/j.commatsci.2003.12.005
24. Cho, J.R., Lee, B.Y., Moon, Y.H., Van Tyne, C.J. (2004), *Investigation of residual stress and post weld heat treatment of multi-pass welds by finite element method and experiments*, J Mater. Proc. Technol. 155-156: 1690-1965. doi: 10.1016/j.jmatprotec2004.04.325
25. Kraedegh, A., Li, W., Sedmak, A., et al. (2017), *Simulation of fatigue crack growth in A2024-T351 T-welded joint*, Struct. Integ. and Life, 17(1): 3-6.
26. Sghayer, A., Grbović, A., Sedmak, A., et al. (2017), *Fatigue life analysis of the integral skin-stringer panel using XFEM*, Struct. Integ. and Life, 17(1): 7-10.